


## ORIGINAL ARTICLE

# Mathematical equations for dental implant stability patterns during the osseointegration period, based on previous resonance frequency analysis studies

Attakorn Charatchaiwanna DDS, MSc<sup>1</sup> |

Thaned Rojsiraphisa PhD, Assistant Professor, Lecturer<sup>2</sup> |

Weerapan Aunmeungtong DDS, PhD, Assistant Professor, Lecturer<sup>1</sup>  |

Peter A. Reichart DDS, Dr.med.dent., Professor<sup>3</sup> |

Pathawee Khongkhunthian DDS, Dr.med.dent., Associate Professor<sup>1</sup> 

<sup>1</sup>Center of Excellence for Dental Implantology, Faculty of Dentistry, Chiang Mai University, Chiang Mai, Thailand

<sup>2</sup>Data Science Research Center, Department of Mathematics, Faculty of Science, Chiang Mai University, Chiang Mai, Thailand

<sup>3</sup>Department of Oral Medicine, Dental Radiology and Oral Surgery, Charité Medical University, Berlin, Germany

## Correspondence

Pathawee Khongkhunthian, Center of Excellence for Dental Implantology, Faculty of Dentistry, Chiang Mai University, Suthep, A. Muang, Chiang Mai 50200, Thailand.  
Email: pathawee@gmail.com

## Funding information

Chiang Mai University research fund

## Abstract

**Background:** Total stability of dental implant can be obtained from resonance frequency analysis (RFA) device, but without primary and secondary stability values.

**Purpose:** To formulate mathematical equations for dental implant stability patterns during the osseointegration period.

**Materials and Methods:** An online systematically search of the literature between January 1996 and December 2017 was performed for all prospective clinical trials that measured implant stability using RFA device during the osseointegration period. Initial mathematical function with adjustable parameters were created. Then curve-fitting was performed using a computerized program to formulate mathematical equations stability patterns.

**Results:** Nine publications (24 study groups) were included in the mathematical analysis. Curve fitting with low sum of squared errors could be applied in all studies, except one. The stability has been divided into high, medium, and low stability. The curve fitting showed stability dip areas and intersection point which predict the returning of the stability to reach the primary stability. The study groups with low primary stability showed the poorest results, the high and medium stability group showed the stability pattern following the assumed primary stability pattern according to the mathematic equations.

**Conclusions:** The model of primary and secondary stability could be predicted from the proposed equations.

## KEYWORDS

dental implant stability, mathematical equation, resonance frequency analysis

## 1 | INTRODUCTION

In the early 1950s, Brånemark<sup>1</sup> performed an experiment to study bone marrow circulation by placing a titanium chamber in a rabbit's bone. As a result of this investigation, he learned that the titanium is duly incorporated within the bone, through a process he later termed osseointegration.<sup>2</sup> Meanwhile, Albrektsson and colleagues examined the interface between implant and bone using electron microscopy, discovering a direct contact interface between bone and implant.<sup>3</sup> Therefore, osseointegration was defined as the direct contact between the implant and the living bone. This histological definition is limited in clinical applications. Zarb and Albrektsson et al<sup>4</sup> suggested a more clinical definition of osseointegration as "a process whereby clinically asymptomatic rigid fixation of alloplastic materials is achieved, and maintained, in bone during functional loading". The rigid fixation indicates that the implant has no clinical mobility when measured using the concept of implant stability.

The measurement of implant stability can be accomplished by a number of techniques, such as removal torque analysis, or pull- and push-through tests, along with histomorphometry. These methods, however, are inadequate for the purposes of long-term clinical assessments because they are invasive, and do not provide the required level of accuracy.<sup>5</sup> To solve this problem, more accurate and non-invasive tests have been introduced, including the Perio-test and Resonance Frequency Analysis (RFA). Doubts remain as to the reliability of the Perio-test because errors can arise when applied by different operators, and the test is not particularly sensitive.<sup>6</sup> As an alternative, RFA was presented via studies involving animals in 1996 by Meredith.<sup>7</sup> The experiment involved an L shaped transducer attached to an implant and set to generate mechanical vibrations at high frequency. By measuring the amplitude and frequency of the signal, the data could be transformed to a value corresponding to the bone-implant interface stiffness.<sup>7</sup> The RFA system used was the Osstell, which generates an implant stability quotient (ISQ) value, which falls in the range of 0 to 100, to measure implant stability. The original Osstell was subsequently replaced with the Osstell Mentor and Osstell ISQ to make non-contact measurements possible through the use of magnetic resonance frequency in order to trigger a magnetic smart peg attached to the implant.<sup>8</sup> RFA is more sensitive and offers a higher resolution than the Perio-test. For this reason, RFA is the method most widely used to measure implant stability.<sup>8</sup>

There are two classifications of implant stability; primary and secondary. Primary stability refers to the initial mechanical stability at the time of implant placement. It arises from the friction derived from the contact between the bone and implant surfaces.<sup>9</sup> Primary stability is influenced by diverse factors, including the design of the implant, the surgical approach used, and the quality of the bone.<sup>10</sup> If primary stability is low, it can result in micromotion of the implant. If this micromotion reaches a level in excess of 50-100  $\mu\text{m}$ , osseointegration may be impaired, and the outcome can be the formation of fibrous tissue, rather than the desired bone, around the implant.<sup>11</sup> Consequently, it is necessary to achieve a high degree of primary stability if

osseointegration is to occur effectively in the case of dental implants. In single implant placement, if primary stability is  $\geq 60$  to 65 ISQ, immediate loading can be applied, with a high survival rate equal to that of conventional loading.<sup>12</sup> However, during the process of implant placement it is possible to cause trauma to the bone and induce bone necrosis around the implant. This leads to the resorption of the traumatized bone and decreases primary stability in the early phase of osseointegration.<sup>9</sup>

Secondary stability is a biological form of stability through bone regeneration and remodeling at the implant-tissue interface.<sup>13</sup> It is possible to separate peri-implant endosseous healing into three stages. The first stage is osteoconduction, whereby the differentiating osteogenic cells migrate toward the surface of the implant, passing through the peri-implant blood clot residue. The blood clots contain fibrin, which is able to support the osteogenic cell migration. The second stage is de novo bone formation, during which a mineralized interfacial matrix forms on the surface of the implant, similar to the cement lines which can be observed in normal bones. The third stage is remodeling of the bone.<sup>14</sup> During the implant healing process, woven bone becomes lamellar bone, resulting in a stronger bone-implant interface and an increase in secondary implant stability.<sup>13</sup> Secondary stability not only depends on the implant healing process, but also on the implant surface condition and on the implant primary stability.<sup>15</sup>

Primary and secondary stability combine into total implant stability. Many studies have recorded total implant stability during the implant healing period, in order to monitor the process of osseointegration.<sup>16-19</sup> A majority of those studies have revealed that implant stability decreases from the baseline, taken as the first day of placement of the implant. Mean stability measures are typically at their minimum during the first 4 weeks, subsequently increasing to become relatively stable. This pattern has been described as a drop, or dip, in implant stability.<sup>16,18</sup>

Corresponding to the behavior of primary and secondary stability, as mentioned above, there is a transitional period of decreasing primary stability and increasing secondary stability. The drop in total implant stability occurs during the transitional period. One study involving animal bones examined the various stages of wound healing around a dental implant, finding that the formation of new bone around the implant took place following the process of resorption.<sup>9</sup> It can thus be inferred that during the healing process, there is a phase in which the initial mechanical implant stability is reduced by osteoclastic activity, but the new bone has not yet sufficiently formed to the point where stability can be maintained.<sup>20</sup> The most significant problem to consider is that if this dip is large, the risk of micromotion rises and there is a higher probability of subsequent failure.<sup>21</sup>

Raghavendra et al<sup>20</sup> proposed a graph of primary and secondary stability which shows an inverse relationship (Figure 1). According to the graph, the overall implant stability, when the implant is first placed, is dependent solely upon mechanical, or primary stability. After the implant has been integrated, total implant stability is based entirely on biological, or secondary stability. The proportional relationship of the influences of primary and secondary stability changes as

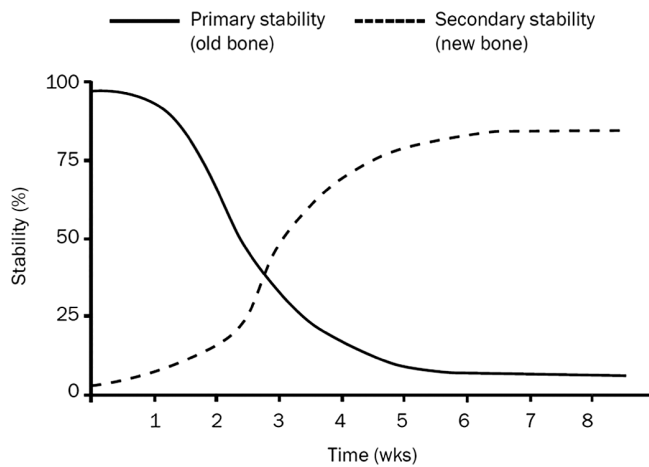


**FIGURE 1** Graph of primary and secondary stability which shows an inverse relationship

the healing process runs its course. However, RFA can measure only total implant stability. It is unable to determine the extent to which the total is affected by primary or secondary inputs. Therefore, from a biological standpoint the relationship between primary and secondary influences remains somewhat open to speculation.

The application of mathematical models to address biological processes is known as biomathematics.<sup>22</sup> In order to resolve biological questions, a biological experiment must be organized, as that the results can be used to create the mathematical model, which connects the various biological variables in the study and determines the parameters relevant to the biological question.<sup>23</sup> Biomathematics is thus a vital tool in the study of various biological fields, such as evolution, immunology, population studies, and areas of neuroscience.<sup>24–28</sup>

Curve fitting is one of the mathematical processes that identifies the curve that best represents a series of points.<sup>28</sup> The curve-fitting function is determined through a process of either smoothing (which results in an approximate fit) or interpolation (which results in an exact fit).<sup>29</sup> The goodness of fit of the resulting function is evaluated through metrics, including the sum of squared errors (SSE) or the sum of squared residuals (SSR).<sup>29</sup> While there are multiple techniques of curve fitting, they have different optimization methods.<sup>28,29</sup> One of the most common curve-fitting approaches is the least squares approach, which optimizes the fit of the regression function by minimizing SSR.<sup>29</sup> Least squares may be used with linear problems (ordinary least squares) or nonlinear or partially nonlinear problems (nonlinear least squares).<sup>29</sup> Curve fitting may use algorithms like the Gauss-Newton algorithm, which is used for nonlinear least squares curve-fitting problems.<sup>29</sup> Curve fitting is commonly used in statistical approaches, including linear and logistic regression.<sup>28,29</sup>

Until now, a mathematical model for implant stability patterns has not been established. However, such a model may describe implant stability during the healing period, in greater depth than currently possible. This study was aimed to formulate mathematical equations for dental implant stability patterns during the osseointegration period, based on previous resonance frequency analysis studies.

## 2 | MATERIALS AND METHODS

### 2.1 | Study selection

The first study on RFA as a method for measuring stability appeared in 1996.<sup>7</sup> Therefore, an online search of the literature between January 1996 to December 2017 was performed using MEDLINE (PubMed) (<https://www.ncbi.nlm.nih.gov/pubmed/>). The following searches were performed using the following key words: dental implant, resonance frequency analysis, and stability(("dental implants"[MeSH Terms] OR ("dental"[All Fields] AND "implants"[All Fields]) OR "dental implants"[All Fields] OR ("dental"[All Fields] AND "implant"[All Fields]) OR "dental implant"[All Fields]) AND ("vibration"[MeSH Terms] OR "vibration"[All Fields] OR "resonance"[All Fields]) AND ("epidemiology"[Subheading] OR "epidemiology"[All Fields] OR "frequency"[All Fields] OR "epidemiology"[MeSH Terms] OR "frequency"[All Fields]) AND ("analysis"[Subheading] OR "analysis"[All Fields]) AND stability[All Fields]).

Study selection was to include all prospective clinical trials that measured dental implant stability using the Osstell mentor device at the time of implant placement and during the osseointegration period (selection criteria shown in Table 1). Titles and abstracts of the searches were initially screened for possible inclusion in the review. If the abstracts contained inadequate information for the decision, the complete paper was obtained and reviewed.

**TABLE 1** Selection criteria

Inclusion criteria	Exclusion criteria
1. Studies published in English	1. Non-English language publications
2. Prospective clinical trials	2. Non-experimental studies (systematic reviews, literature reviews, and meta-analyses)
- Human participants older than 18 years with no systemic disease or contributing factors that affect osseointegration of dental implants.	3. Case reports
3. Treatment using root-form implants	4. In vitro studies
4. Osstell magnetic device used to measure implant stability (measured in terms of ISQ 1–100 using magnetic frequencies by connecting the implant to Smartpeg)	5. Animal studies
5. Implant stability measured:	6. Treatment using non-root-form implant (orthodontic mini-screws, palatal implants, etc.)
- At time of implant placement	7. Insufficient points of implant stability
- At least four times in the first 6 weeks	• Not measured at time of implant placement
- At least two times between the 7th and 13th weeks	• Measured fewer than four times in the first 6 weeks
6. Mean ISQ value and standard deviation shown at all measured times	• Measured fewer than two times between the 7th and 13th weeks
7. Complete paper accessible	8. Mean ISQ value and standard deviation not shown at all measured times
	9. Completed paper not accessible

Abbreviations: ISQ, implant stability quotient.

## 2.2 | Mathematical model

A mathematical function to determine implant stability was used according to the biological point of view as mentioned above. The curve for total implant stability (recorded from the evaluated studies) is derived from two curves. The first is based on primary stability, which is a downward trend. The curve of the graph for primary implant stability begins with the implant stability which is recorded after surgery (day 0) and continues to decrease subsequently. The second curve is based on secondary stability, which is an upward trend (starting from 0 on the day of surgery and continuing to increase). These two curves were presumed and were demonstrated as a sigmoid curve.<sup>20</sup> Therefore, the mathematical function used in this study was the sigmoid function:  $y = \frac{1}{1+e^{-t}}$ , where  $y$  refers to implant stability and  $t$  refers to time.

To control the range of stability, we added two parameters ( $c_1$  and  $c_2$ ) into the sigmoid function, which the modified function into the form  $y = c_1 + \frac{c_2 - c_1}{1 + \left(\frac{t}{c_3}\right)^{c_4}}$ . If  $c_1 < c_2$ , the graph shows a downward trend with  $c_1$  and  $c_2$  are the lower and upper range of stability, respectively (Figure 2A). On the other hand, if  $c_1 > c_2$ , the graph shows an upward trend with  $c_1$  and  $c_2$  are the upper and lower range of stability, respectively (Figure 2B).

In be able to vary the slope and pattern of the graph, we added two more parameters ( $c_3$  and  $c_4$ ) and replaced  $e^{-t}$  with  $\frac{t}{c_3}$ . Therefore, we had flexibility in choices of parameters to fit both linear and nonlinear patterns, as shown in Figure 3 as an example.

Therefore, in this study, we used the modified sigmoid function in the form

$$y = c_1 + \frac{c_2 - c_1}{1 + \left(\frac{t}{c_3}\right)^{c_4}},$$

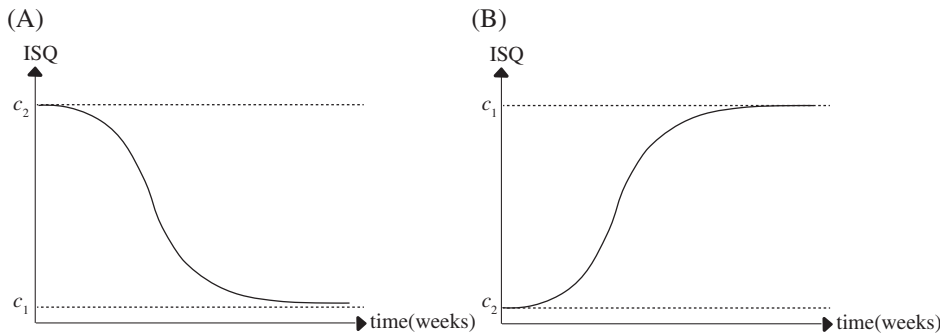


**FIGURE 2** Modified sigmoid functions with downward trend (a) and upward trend (b)

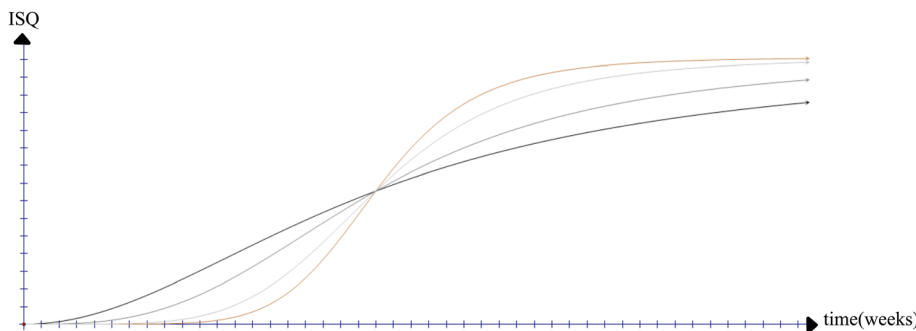


**FIGURE 3** Graphs of modified sigmoid function with various choices of  $c_3$  and  $c_4$

where  $y$  refers to implant stability (Osstell units range from 1 to 100),  $t$  refers to time (weeks) and  $c_1, c_2, c_3, c_4$  are parameters that can be adjusted to fit the data.

## 2.3 | Curve-fitting with results from selected studies

This study used data from selected studies which recorded implant stability by RFA during osseointegration periods. The means of implant stability were used to fit with the mathematical model mentioned above. Implant stability in the selected studies referred to the total implant stability (denoted by TS) as the sum of the two curves.

The first curve showed a downward trend corresponding to primary stability behavior (denoted by PS). The equation used for curve-fitting was

$$PS = p_1 + \frac{p_2 \cdot p_1}{1 + \left(\frac{t}{p_3}\right)^{p_4}}.$$

The upper range in the downward trend represented stability that was recorded at the surgical visit (called baseline and denoted by SB) and the lower range was zero. Therefore, the parameter  $p_1$  was fixed at 0, and  $p_2$  was fixed to SB. So, the equation used for curve-fitting was

$$PS = \frac{SB}{1 + \left(\frac{t}{p_3}\right)^{p_4}}.$$

The second curve showed an upward trend corresponding to secondary stability (denoted by SS) behavior. The equation was the same as for the first curve with different parameters that were changed to  $s_1, s_2, s_3$ , and  $s_4$ . The upper range of the curve represented stability that was recorded at the final observation period (called final stability

and denoted by SF) and the lower range was zero. Therefore, the parameter  $s_1$  was fixed to SF and  $s_2$  was fixed to 0. So, the equation used for representing secondary stability was

$$SS = SF - \frac{SF}{1 + \left(\frac{t}{s_3}\right)^{s_4}}.$$

The equation used to fit mean total implant stability (data from selected studies), was the sum of the two equations above:

$$TS = \frac{SB}{1 + \left(\frac{t}{p_3}\right)^{p_4}} + \left\{ SF - \frac{SF}{1 + \left(\frac{t}{s_3}\right)^{s_4}} \right\},$$

where TS refers to total implant stability recorded by RFA (Osstell units),  $t$  refers to time (weeks) and  $p_3$ ,  $p_4$ ,  $s_3$ ,  $s_4$  are parameters that could be adjusted. Curve fitting was performed using Minitab 17 (Statistical Software, 2010, Minitab Inc., State College, Pennsylvania). A Gauss-Newton algorithm was applied to find a set of parameters that minimized the sum of squared errors (SSE).

## 2.4 | Analysis of the equations

From the best-fit equation above, these following subjects were analyzed:

a. The intersection point (denoted by  $t^*$ ) between the fitted equation and baseline. The intersection point showed the time at which the total implant stability returned to the baseline by calculating the  $t^*$  value from the equation:

$$SB = \frac{SB}{1 + \left(\frac{t^*}{p_3}\right)^{p_4}} + SF - \frac{SF}{1 + \left(\frac{t^*}{s_3}\right)^{s_4}}.$$

a. The area between two functions (total implant stability equation and baseline). This indicated the area of the stability dip from the time of implant placement to the time when total implant stability returned to the baseline. It was calculated from the equation:

$$\text{Area between two functions} = \int_0^{t^*} (SB - TS) dt.$$

In case that  $t^*$  could not be calculated, the final observation period was used instead.

## 3 | RESULTS

The initial search yielded 533 publications found in PubMed/Medline. All of the papers were screened by considering the formal inclusion and exclusion criteria. A total of 506 papers were excluded on the basis of the article titles and/or the abstracts. As a result, 27 publications were considered for full-text analysis. Following a discussion after the full-text analysis, 18 studies were excluded (2 studies with full papers that could not be accessed, 3 studies that used the Osstell integration electronic device, and 13 studies that did not show the ISQ value at all measurement points). Finally, nine studies were included in the mathematical analysis. The search strategy and the results of the identification, screening and inclusion of the publications are described in Figure 4.

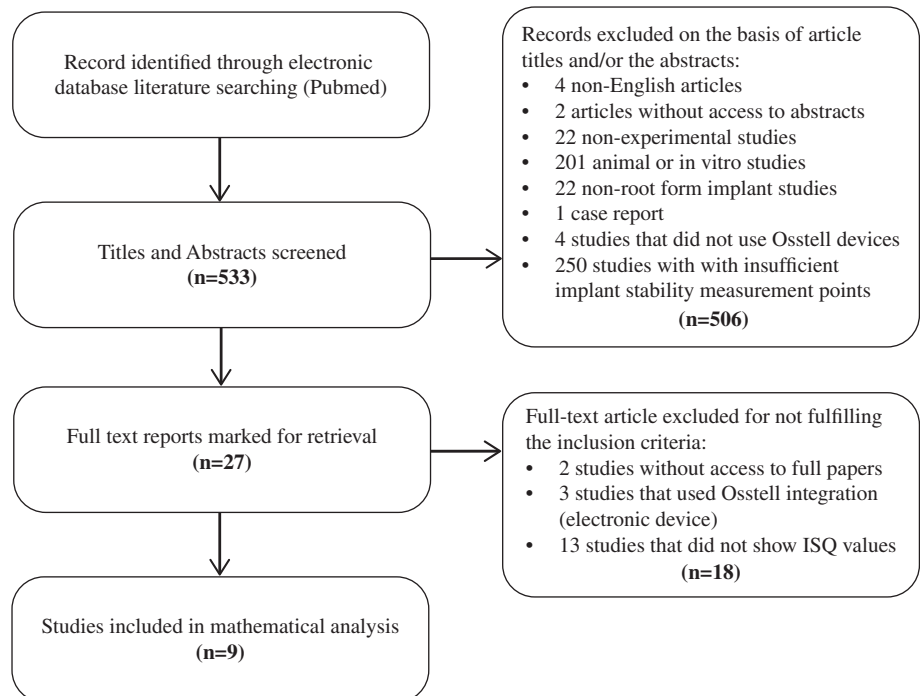


**FIGURE 4** Search strategy and results of identification, screening, and inclusion of publications for mathematical analysis

**TABLE 2** Overview of the data from the nine studies included for mathematical analysis

Author	Study group number	Implant system (as reported by the authors)	Surface	Size	Surgical technique	Loading protocol	Bone quality	Site	Direction of measurement	N
Gu et al <sup>18</sup>	1	Straumann Standard Plus	SLA	Unclarified	Summers TSFE without graft	Conventional	Unclarified	Posterior Maxilla	Three way (B, Li, D)	35
	2	PW Plus	Sandblast and acid etch	5 × 10	Drilling	Conventional	2,3 (Lekhom)	Lower molar	Two way (B M)	10
Stacchi et al <sup>31</sup>	3.1	Biomet 3i	Dual acid etch with deposition of calcium phos phate	4 × 10	Drilling	Conventional	Unclarified	Upper premolar	Three way (B, Li, D)	20
	3.2				Piezosurgery					19
Shokri et al <sup>17</sup>	4	ITI implants	SLA-coated	Unclarified	Drilling	Conventional	D2 or D3 (Friborg)	Mandible	One way (B)	15
Marković et al <sup>32</sup>	5.1	BlueSkyBredent	Self-tap	4 × 10	Condensing	Conventional	3,4(Lekhom)	Posterior maxilla	One way (B)	28
	5.2	Straumann	Non-self tap	4.1 × 10	Condensing					26
	5.3	BlueSkyBredent	Self-tap	4 × 10	Drilling					28
	5.4	Straumann	Non-self tap	4.1 × 10	Drilling					24
Simunek et al <sup>33</sup>	6.1	Bio, Impladent	Alkali-treated surface	3.7 × 16	Drilling	Immediate load	1, 2, 3 (Lekhom)	Anterior mandible	Two way (B M)	46
	6.2									29
	6.3									15
Liaje et al <sup>34</sup>	7.1	Straumann	SLActive	3.5-5 × 9-15	Drilling	Early load (8 week)	2, 3 (Lekhom)	All	Three way (B, Li, D)	23
	7.2	Astratech	Fluoride treat							28
	7.3	Thommen	Sandblast thermal acid etch							24
Han et al <sup>35</sup>	8.1	Straumann tissue level	SLA	4.1 × 10	Drilling	Conventional	Unclarified	22 posterior, 1 anterior	Three way (B, Li, D)	10
	8.2		SLActive	4.1 × 10						8
	8.3		SLA	4.8 × 10						5
Sim et al <sup>31</sup>	9.1	Straumann tissue level	SLA	4.1 × 8	Drilling	Conventional	All	Posterior region	Two way (B O)	16
	9.2			4.1 × 10			All		Two way (B O)	16
	9.3			4.1 × 8.10			All	B		32
	9.4			4.1 × 8.10			All	O		32
	9.5			4.1 × 8.10			2 (Lekhom)		Two way (B O)	14
	9.6			4.1 × 8.10			3, 4 (Lekhom)		Two way (B O)	16



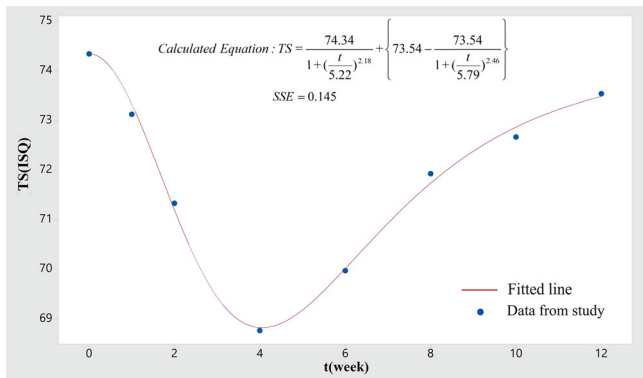


**FIGURE 5** Example of fitted line plot with low sum of squared errors (SSE) (data were adopted from Marković et al<sup>32</sup>)

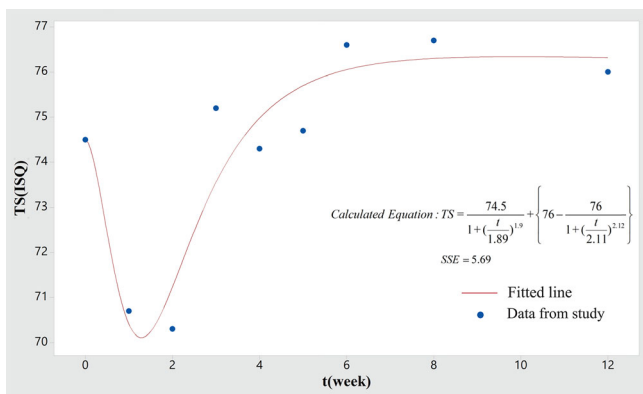


**FIGURE 6** Example of fitted line plot with high sum of squared errors (SSE) (data were adopted from Sim and Lang<sup>30</sup>)

Of the 9 papers that met the inclusion criteria, 3 had one clinical study group and the other 6 each had multiple study groups, resulting in a total of 24 study groups. The implant system, surface design, implant size, surgical technique, loading protocol, bone quality, surgical site, direction of measurement, and number of implants in each study are shown in Table 2. Data from these 24 study groups were analyzed using the modified sigmoid function. The data in 18 study groups from 8 papers were closely fit with the modified sigmoid function (low SSE ranging from 0.05 to 1.733, example shown in Figure 5) but the data in 6 study groups from one paper<sup>31</sup> were fit with high SSE, ranging from 2.58 to 19.18 (example shown in Figure 6). Calculated parameters of the equations ( $p_3$ ,  $p_4$ ,  $s_3$ , and  $s_4$ ), stability dip areas, intersection points, baselines, and final implant stability are shown in Table 3. Owing to the heterogeneity of the various study results, they were categorized into three main groups according to the primary stability at the surgical visits (baseline). Based on the ISQ scale, high stability means  $>70$  ISQ, between 60 and 69 is medium stability and  $<60$  ISQ is considered as low stability (Figure 7).<sup>36–44</sup> These three groups were named as Group H (high primary stability), M (medium primary stability), and L (low primary stability), respectively.

### 3.1 | Total stability graphs and intersection points

The 24 total stability graphs from Groups H, M, and L are shown in Figures 8–9, and 10, respectively. Most of them show a dropping pattern (stability dip). However, two graphs in Group M and two graphs in Group L show increasing patterns of total stability throughout the observation periods. In Group H, which consisted of 17 study groups, 8 of the 17 curves had no intersection point in the observation periods because total implant stability did not reach the baseline; on the other hand, 9 of 17 had intersection points in a range from 3.59 to 9.56 weeks. In Group M (five study groups), three curves had intersection points in a range from 3.19 to 5.06 weeks, but two had no intersection point due to total implant stability being higher than baseline in all of the observation periods. The latter finding is the same as that in the single study in Group L (two study groups). A summary of all intersection points is shown in Figure 11.

### 3.2 | Stability dip areas

A summary of the stability dip areas in all three groups are plotted in Figure 12. A positive stability dip area indicates that total implant stability has a dropping pattern below the baseline; conversely, a negative stability dip area indicates that total implant stability is higher than the baseline. In Group H, all of the total implant stability curves had positive stability dip areas, which ranged from 4.44 to 61.322 week.ISQ. In Group M, three of five curves had positive stability dip areas which ranged from 6.69 to 6.99 week.ISQ, but the other two stability dip areas were negative (–70.79 and –82.28 week.ISQ). Both curves in Group L had negative stability dip areas (–140.51 and –153.51 week.ISQ).

### 3.3 | Primary and secondary stability graphs

Based on modified sigmoid function, we obtained primary and secondary stability curves as shown in Figures 13 and 14, respectively. One can notice that all of Group H and some of Group M showed a rapid drop in primary stability in the first 6 weeks. On the other hand, primary stability remained constant in the others in Group M and in both in Group L, for 12 weeks before dropping. For secondary stability, all of Group H and some of Group M showed exponential increases, whereas the rest showed slow increases.

## 4 | DISCUSSION

Implant stability has been described as a critical factor for treatment success during the osseointegration period.<sup>45</sup> Primary stability comes from implant design, bone quality, the difference between the implant bed and implant size and the friction between implant surface and bone. Secondary stability is assumed to represent the biological phenomena of osseointegration.<sup>10,13</sup> The drop in implant stability is defined as the destructive inflammatory reaction during early bone-implant healing.<sup>9</sup> Maintenance

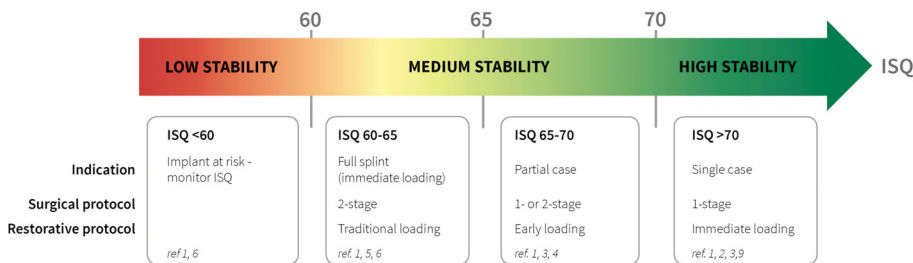
**TABLE 3** Calculated parameters of equations ( $p_3$ ,  $p_4$ ,  $s_3$ , and  $s_4$ ), stability dip areas, intersection points, baseline, final implant stability, and SSE

Study group number	Baseline	Final	Dip area	Inter-section	$p_3$	$p_4$	$s_3$	$s_4$	SSE
1	70.1	72.8	8.71	6	4.737	2.358	5.03	2.584	0.1128
2	77	79.6	32.06	6.56	0.929	0.859	1.7	1.1	1.7335
3.1	72.2	69.2	61.322	<sup>a</sup>	6.864	1.125	8.08	1.374	0.1864
3.2	70.5	71.0	8.8028	9.56	5.383	1.231	5.67	1.315	0.1645
4	77.2	75.6	33.34	<sup>a</sup>	5.465	2.287	5.93	2.54	0.5723
5.1	74.34	73.54	35.06	<sup>a</sup>	5.222	2.175	5.79	2.454	0.1449
5.2	74.03	71.88	40.88	<sup>a</sup>	3.243	2.516	3.6	2.646	0.1445
5.3	65.1	68.20	6.73	5.06	3.764	3.01	4.02	3.204	0.4715
5.4	61.2	67.10	6.99	3.96	3.49	1.984	3.87	2.278	0.9293
6.1	76.6	74.8	13.09	<sup>a</sup>	1.892	2.721	1.93	2.918	0.0539
6.2	70.2	71.5	4.44	4.36	2.367	0.861	2.61	0.929	0.1818
6.3	64.1	69.7	6.69	3.19	2.739	1.299	3.15	1.535	0.0803
7.1	78.39	76.17	18.68	<sup>a</sup>	2.21	2.541	2.32	2.635	0.0504
7.2	76.57	74.79	18.57	<sup>a</sup>	2.91	2.167	3.1	2.304	0.1021
7.3	75.13	71.5	28.7	<sup>a</sup>	2.39	2.479	2.56	2.591	0.0091
8.1	72.4	76.5	5.8	5.14	3.341	3.984	3.57	3.834	0.2219
8.2	75.7	78.8	14.52	6.83	5.647	1.421	6.13	1.657	1.5233
8.3	74.4	77.8	12.48	5.19	3.373	2.046	3.76	2.293	1.4952
9.1	59.8	74.6	-140.51	<sup>b</sup>	16.64	7.873	58.2	0.679	2.5805
9.2	70.3	74.8	6.24	4.53	4.356	1.605	4.69	1.788	4.7267
9.3	64.5	74.6	-82.28	<sup>b</sup>	19.56	6.183	65.9	0.909	2.6491
9.4	65.7	74.8	-70.79	<sup>b</sup>	19.57	2.662	19.8	1.609	3.7747
9.5	74.5	76	8.41	3.59	1.893	1.9	2.11	2.122	5.6875
9.6	56	74	-153.51	<sup>b</sup>	13.28	26.39	68.4	0.603	19.177

Abbreviation: SSE, sum of squared errors.

<sup>a</sup>No intersection points in the observation period because total implant stability did not reach the baseline.

<sup>b</sup>No intersection points in the observation period due to total implant stability graph being higher than the baseline in all of the observation periods.

**FIGURE 7** This graphic depicts implant stability quotient (ISQ) values as they relate to implant stability (Courtesy of Osstell)

of high implant stability during osseointegration permits immediate implant loading after the surgical implant placement. The use of mathematical equations may permit prediction of implant stability during the healing period. Hence, optimal timing of loading an implant can be determined.

#### 4.1 | Total implant stability and calculated equations

Formulation of the equations for implant stability during the healing period was performed using curve fitting. The modified sigmoid function could be closely fit to total implant stability from

most studies. However, one study<sup>30</sup> showed irregular patterns or no dropping pattern (stability dip) of total implant stability. Those patterns were the reason why the equations in this study could not be fit properly, and why the calculated SSE was high.

The dropping pattern of total implant stability was found only in study groups with high to medium primary implant stability. However, implants with medium to low primary stability showed an increasing pattern over the healing periods. This result corresponds with that of the clinical study of Nedir et al.<sup>46</sup>

The parameter values ( $p_3$ ,  $p_4$ ,  $s_3$ , and  $s_4$ ) in the equations were not equal in any of the 24 equations, nor were the stability dip areas or



**FIGURE 8** Total stability graph from Group H (baseline: >70; 17 curves)

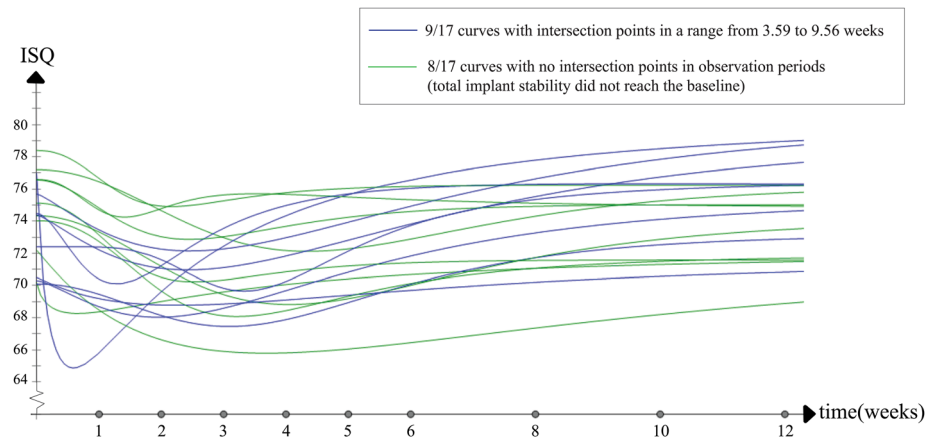


**FIGURE 9** Total stability graph from Group M (baseline: 60-70; five curves)

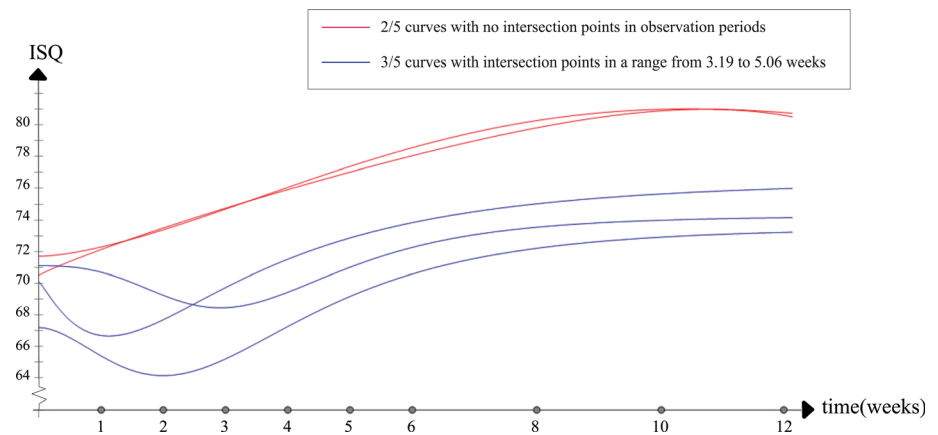
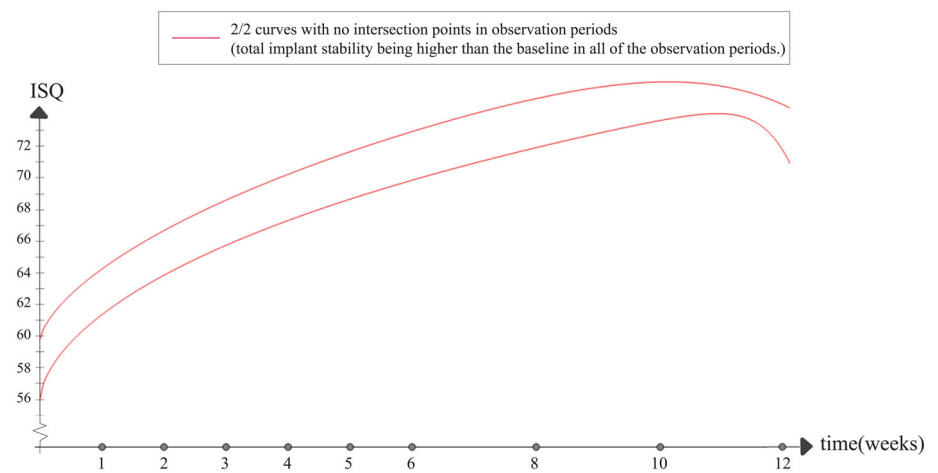


**FIGURE 10** Total stability graph from Group L (baseline: <60; two curves)



the intersection points. These differences may be caused by various factors, such as implant design, surgical technique, the implant surface, different study designs, and so on.

## 4.2 | Intersection points

Group H tended to have higher intersection points than Group M (Figure 11). This means that for implants with high primary stability, implant stability tends to increase from the lowest dropping point and reach the baseline slower than those implants with medium primary

stability. Furthermore, sometimes stability in Group H did not increase to reach the baseline in the first 12 weeks. This finding is consistent with the study from Friberg and colleagues, who found that the stability of implants placed in softer bone seemed to catch up with that of those placed in denser bone sites.<sup>47</sup>

## 4.3 | Stability dip areas

The calculated stability dip areas from the equations showed the amount of the dropping of the total implant stability from the

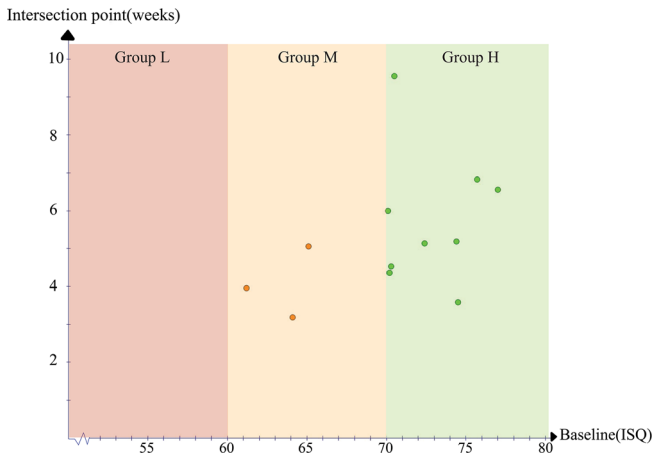


**FIGURE 11** Plot of intersection points vs baseline

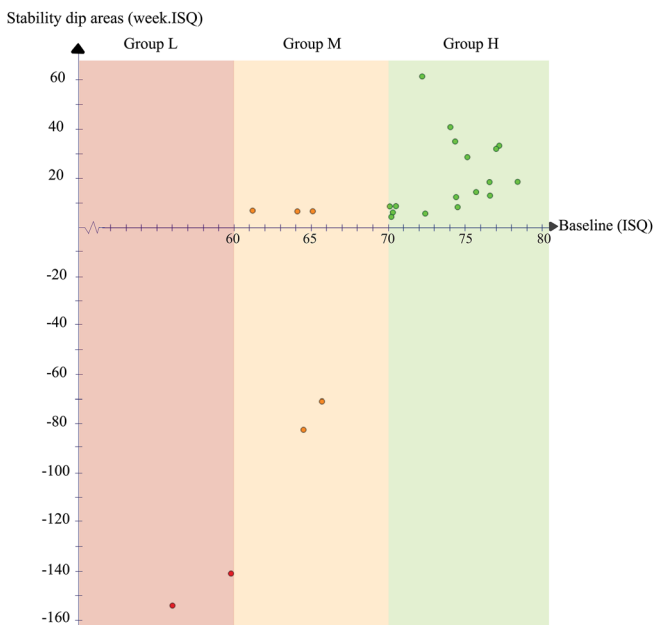


**FIGURE 12** Plot of stability dip areas vs baseline

baseline. In Group H, with a dropping pattern of total implant stability, there was a wide range in the values of the stability dip areas, all positive. In contrast, some study groups in Group M and both in Group L showed negative stability dip areas because the total implant stability

increased from the first week with no dropping below the baseline during the healing periods. A greater negative value may indicate a higher rate of bone formation than of bone resorption around the implant. After comparing these values in the three main groups, the stability dip areas in Group H were mostly higher than those in both Group M and Group L. The most significant problem to consider is that if the dip is large, especially in implants with high primary stability, the risk of micromotion increases and there is an increased probability of subsequent failure.<sup>21</sup> Nevertheless, the lowest dropping point in mean implant stability in this group was still higher than 65, which suggests that the implant can be immediately loaded.<sup>48</sup>

The term “osseous pressure necrosis” is used frequently in the dental literature and is defined by researchers as excessive compression of, or pressure on, bone that is created during implant insertion.<sup>49,50</sup> Compression of bone beyond its physiological limits may result in ischemia, which can lead to osseous necrosis. Higher primary stability causes more pressure on bone and may result in increased bone necrosis and resorption during the beginning phase of healing. Such increased bone necrosis and resorption may be the reasons that the calculated stability areas in Group H were higher than in the other groups, and that total implant stability returned to the baseline more slowly. The primary stability curves plotted from the calculated equations also showed that the primary stability in Group H tended to drop more quickly than that in Group M and Group L (Figure 13). This rapid drop in primary stability may imply that the bone resorption is increased with implants with high primary stability.

#### 4.4 | Primary and secondary implant stability

To analyze the trend of bone resorption and formation, we further investigated the relation of the difference between primary and secondary stability, as in the equation:  $DB = (SB - PS) - SS$ , where DB denotes the difference between bone resorption and bone formation.

In the study groups with the dropping graph pattern of total implant stability (all study groups in Group H and two study groups in Group M), DB was positive in the early phase and became negative later (example shown in Figure 15). This implies that the rate of bone resorption was greater than that of bone formation at beginning phase and then it became less. These results are consistent with the observed behavior of the primary and secondary stability obtained

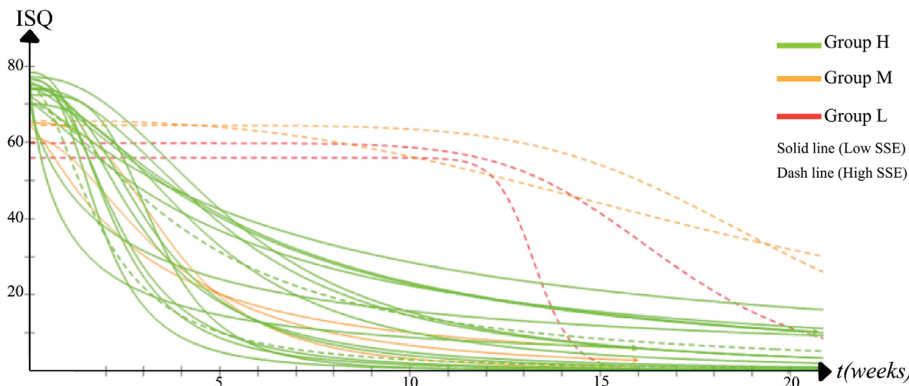


**FIGURE 13** Modified sigmoid functions of primary stability

**FIGURE 14** Modified sigmoid functions of secondary stability

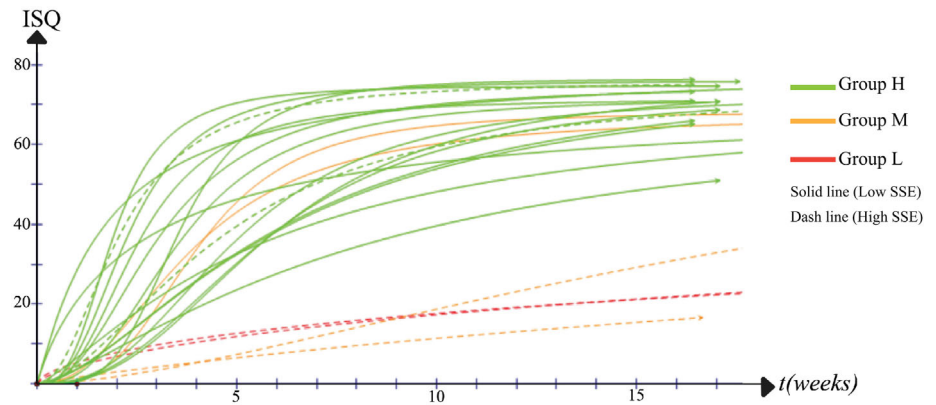


**FIGURE 15** Example of SB-PS and SS in study groups with a dropping graph pattern of total implant stability

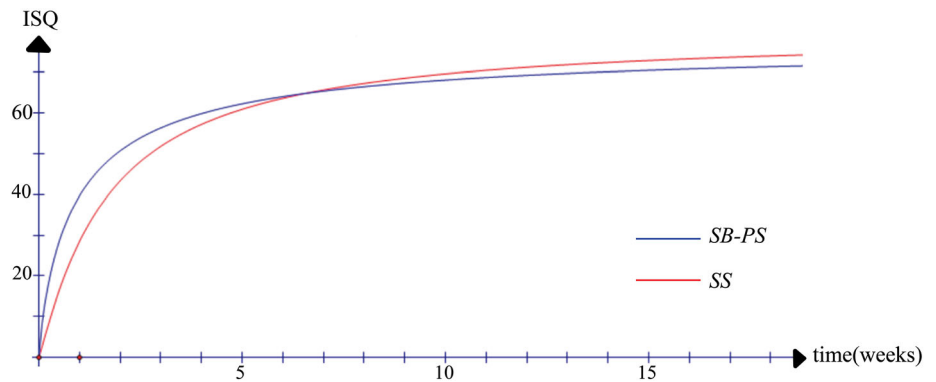
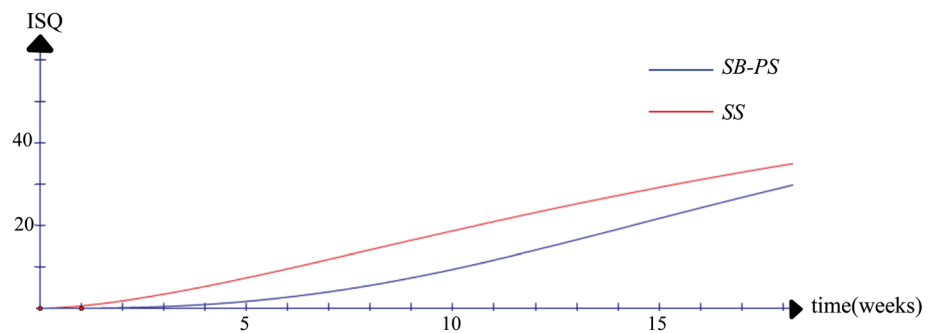


**FIGURE 16** Example of SB-PS and SS in study groups with an increasing patterns of total implant stability



from an experiment with animals, in which the new bone formation around an implant occurred after the resorption process.<sup>9</sup>

In contrast, in study groups with an increasing pattern of total implant stability (two study groups in Group M and both study groups in Group L), DB was always negative (example shown in Figure 16) implying that the rate of bone formation is greater than that of bone resorption throughout the healing period.

From the modified sigmoid function used in this study, we observed that if  $p_3$  and  $p_4$  were close to  $s_3$  and  $s_4$ , respectively, primary and secondary stability were more likely to be a vertical reflection with nearly zero stability dip areas. Biologically, this can be done by speeding up the bone formation rate to be as close to the bone resorption rate as possible. Clinically, implants with high primary stability and low stability dip areas are preferable, and immediate loading

can be applied with low risk of micromotion and fibrous tissue formation.<sup>11</sup> With Digital CAD/CAM technology, the restoration can be accurately fabricated and rapidly immediately placed after placement of the implant.<sup>51</sup> However, this study showed that calculated stability dip areas increased in implants with high primary stability. Additional clinical studies are required to confirm this finding.

From the results of this study, it can be clinically implemented as follows, the stability of implants will be weakest at the first 2-4 weeks after the surgical placement, any conditions that will produce the micromotion of the implant, for example, tightening of the healing abutment, should be avoided. The implants with low stability ( $ISQ < 60$ ) should leave longer before attaching to the prosthesis (more than 2 months).

## 4.5 | Limitations of the study

- The equations were calculated using mean total implant stability; therefore, one equation cannot generally represent all individual cases, but each case can be represented by this proposed modified sigmoid function by adjusting the parameters  $p_3$ ,  $p_4$ ,  $s_3$ , and  $s_4$ .
- There were only two study groups in Group L and five study groups in Group M that met the inclusion criteria. Furthermore, the modified sigmoid function could not be fit properly in most of them; hence the proposed primary, secondary, and total implant stability in these groups may not have presented correctly.

## 5 | CONCLUSION

Mathematical models are useful tools for calculating stability dip areas and intersection points. The patterns of primary and secondary stability may also be predicted and help us to understand the processes of bone resorption and bone formation more clearly. The equations may be used to for improve future implant design for immediate loading procedure using together with digital implant Dentistry. In all the included studies, the calculated equations were different, as were the stability dip areas and intersection points. These differences may be caused by various factors in different study designs. Further, well-randomized, control trials are required to confirm the proposed equations.



## ACKNOWLEDGEMENTS

The authors would like to thank Dr. M. Kevin O Carroll, Professor Emeritus of the University of Mississippi School of Dentistry, USA, and Faculty Consultant at Chiang Mai University Faculty of Dentistry, Thailand, for participated in technical editing of the manuscript. This study was supported by Chiang Mai University research fund.

## CONFLICT OF INTEREST

The authors declare no potential conflict of interest.

## ORCID

Weerapan Aunmeungtong  <https://orcid.org/0000-0003-4302-8671>  
 Pathawee Khongkhunthian  <https://orcid.org/0000-0002-5994-4482>

## REFERENCES

1. Brånemark P-I. Vital microscopy of bone marrow in rabbit. *Scand J Clin Lab Invest*. 1959;11:1.
2. Brånemark P-I. Osseointegration and its experimental background. *J Prosthet Dent*. 1983;50(3):399-410.
3. Albrektsson T, Brånemark P-I, Hansson H-A, Lindström J. Osseointegrated titanium implants: requirements for ensuring a long-lasting, direct bone-to-implant anchorage in man. *Acta Orthop Scand*. 1981;52(2):155-170.
4. Zarb G, Albrektsson T. Osseointegration: a requiem for the periodontal ligament. *Int J Periodont Rest Dent*. 1991;11(1):88-91.
5. Al-Jetaily S, Al-dosari AA. Assessment of Ostell™ and Periotest® systems in measuring dental implant stability (in vitro study). *Saudi Dent J*. 2011;23(1):17-21.
6. Salvi GE, Lang NP. Diagnostic parameters for monitoring peri-implant conditions. *Int J Oral Maxillofac Implants*. 2004;19(7):116-127.
7. Meredith N, Alleyne D, Cawley P. Quantitative determination of the stability of the implant-tissue interface using resonance frequency analysis. *Clin Oral Implants Res*. 1996;7(3):261-267.
8. Sachdeva A, Dhawan P, Sindwani S. Assessment of implant stability: methods and recent advances. *Br J Med Med Res*. 2016;12(3):1-10.
9. Berglundh T, Abrahamsson I, Lang NP, Lindhe J. De novo alveolar bone formation adjacent to endosseous implants. *Clin Oral Implants Res*. 2003;14(3):251-262.
10. Manzano-Moreno FJ, Herrera-Briones FJ, Bassam T, Vallecillo-Capilla MF, Reyes-Botella C. Factors affecting dental implant stability measured using the Ostell Mentor Device: a systematic review. *Implant Dent*. 2015;24(5):565-577.
11. Brunski JB. The influence of force, motion and related quantities on the response of bone to implants. In: Fitzgerald R, ed. *Non Cemented Total Hip Arthroplasty*. New York, NY: Raven Press; 1988:7-10.
12. Benic GI, Mir-Mari J, Hämmerle F, Christoph H. Loading protocols for single-implant crowns: a systematic review and meta-analysis. *Int J Oral Maxillofac Implants*. 2014;29:222-238.
13. Cochran D, Schenk R, Lussi A, Higginbottom F, Buser D. Bone response to unloaded and loaded titanium implants with a sandblasted and acid-etched surface: a histometric study in the canine mandible. *J Biomed Mater Res*. 1998;40(1):1-11.
14. Davies J. Mechanisms of endosseous integration. *Int J Prosthodont*. 1998;11(5):391-401.
15. Atsumi M, Park S-H, Wang H-L. Methods used to assess implant stability: current status. *Int J Oral Maxillofac Implants*. 2007;22(5):743-754.
16. Lai HC, Zhang ZY, Wang F, Zhuang LF, Liu X. Resonance frequency analysis of stability on ITI implants with osteotome sinus floor elevation technique without grafting: a 5-month prospective study. *Clin Oral Implants Res*. 2008;19(5):469-475.
17. Shokri M, Daraeighadikolaei A. Measurement of primary and secondary stability of dental implants by resonance frequency analysis method in mandible. *Int J Dent*. 2013;2013:1-5.
18. Gu YX, Shi JY, Zhuang LF, Qian SJ, Mo JJ, Lai HC. Transalveolar sinus floor elevation using osteotomes without grafting in severely atrophic maxilla: a 5-year prospective study. *Clin Oral Implants Res*. 2016;27(1):120-125.
19. Tirachaimongkol C, Pothacharoen P, Reichart PA, Khongkhunthian P. Relation between the stability of dental implants and two biological markers during the healing period: a prospective clinical study. *Int J Implant Dent*. 2016;2(1):27.
20. Raghavendra S, Wood MC, Taylor TD. Early wound healing around endosseous implants: a review of the literature. *Int J Oral Maxillofac Implants*. 2005;20(3):425-431.
21. Alam MN, Anand N, Chandrasekaran S, Kovendhan Y. Is primary stability the gold standard factor in implant success. *Dent Hypotheses*. 2014;5(2):70.
22. Shonkwiler RW, Herod J. *Mathematical Biology: An Introduction with Maple and Matlab*. Vol 1. London, New York, NY: Springer Dordrecht, Heidelberg; 2009.
23. Friedman A. What is mathematical biology and how useful is it. *Notice AMS*. 2010;57(7):851-857.
24. Craciun G, Brown A, Friedman A. A dynamical system model of neurofilament transport in axons. *J Theor Biol*. 2005;237(3):316-322.
25. Yunes RA. The evolution of the human mind and logic-mathematics structures. *J Theor Biol*. 2005;236(1):95-110.

26. Kumar PS, Saravanan A, Kumar KA, Yashwanth R, Visvesh S. Removal of toxic zinc from water/wastewater using eucalyptus seeds activated carbon: non-linear regression analysis. *IET Nanobiotechnol.* 2016;10(4):244-253.
27. Emerick B, Singh A. The effects of host-feeding on stability of discrete-time host-parasitoid population dynamic models. *Math Biosci.* 2016;272:54-63.
28. Seber GA, Lee AJ. *Linear Regression Analysis.* Auckland, New Zealand: John Wiley & Sons; 2012.
29. Hansen PC, Pereyra V, Scherer G. *Least Squares Data Fitting with Applications.* Baltimore, MD: Johns Hopkins University Press 2013.
30. Sim CP, Lang NP. Factors influencing resonance frequency analysis assessed by Osstell™ mentor during implant tissue integration: I. Instrument positioning, bone structure, implant length. *Clin Oral Implants Res.* 2010;21(6):598-604.
31. Stacchi C, Vercellotti T, Torelli L, Furlan F, Di Lenarda R. Changes in implant stability using different site preparation techniques: twist drills versus Piezosurgery. A single-blinded, randomized, controlled clinical trial. *Clin Implant Dent Relat Res.* 2013;15(2):188-197.
32. Marković A, Calvo-Guirado JL, Lazić Z, et al. Evaluation of primary stability of self-tapping and non-self-tapping dental implants. A 12-week clinical study. *Clin Implant Dent Relat Res.* 2013;15(3):341-349.
33. Simunek A, Kopecka D, Brazda T, Strnad J, Capek L, Slezak R. Development of implant stability during early healing of immediately loaded implants. *Int J Oral Maxillofac Implants.* 2012;27(3):619-627.
34. Liaje A, Ozkan YK, Ozkan Y, Vanlıoğlu B. Stability and marginal bone loss with three types of early loaded implants during the first year after loading. *Int J Oral Maxillofac Implants.* 2012;27(1):162-172.
35. Han J, Lulic M, Lang NP. Factors influencing resonance frequency analysis assessed by Osstell™ mentor during implant tissue integration: II. Implant surface modifications and implant diameter. *Clin Oral Implants Res.* 2010;21(6):605-611.
36. Sennerby L. Jahre Erfahrung mit der Resonanzfrequenzanalyse. *Implant Dent.* 2013;21(1):21-33.
37. Kokovic V, Jung R, Feloutzis A, Todorovic VS, Jurisic M, Hämmerle CH. Immediate vs. early loading of SLA implants in the posterior mandible: 5-year results of randomized controlled clinical trial. *Clin Oral Implants Res.* 2014;25(2):e114-e119.
38. Bornstein MM, Hart CN, Halbritter SA, Morton D, Buser D. Early loading of nonsubmerged titanium implants with a chemically modified sand-blasted and acid-etched surface: 6-month results of a prospective case series study in the posterior mandible focusing on peri-implant crestal bone changes and implant stability quotient (ISQ) values. *Clin Implant Dent Relat Res.* 2009;11(4):338-347.
39. Baltayan S, Pi-Anfruns J, Aghaloo T, Moy PK. The predictive value of resonance frequency analysis measurements in the surgical placement and loading of endosseous implants. *J Oral Maxillofac Surg.* 2016;74(6):1145-1152.
40. Östman PO, Hellman M, Sennerby L. Direct implant loading in the edentulous maxilla using a bone density-adapted surgical protocol and primary implant stability criteria for inclusion. *Clin Implant Dent Relat Res.* 2005;7:s60-s69.
41. Rodrigo D, Aracil L, Martin C, Sanz M. Diagnosis of implant stability and its impact on implant survival: a prospective case series study. *Clin Oral Implants Res.* 2010;21(3):255-261.
42. Pagliani L, Sennerby L, Petersson A, Verrocchi D, Volpe S, Andersson P. The relationship between resonance frequency analysis (RFA) and lateral displacement of dental implants: an in vitro study. *J Oral Rehabil.* 2013;40(3):221-227.
43. Trisi P, Carlesi T, Colagiovanni M, Perfetti G. Implant stability quotient (ISQ) vs direct in vitro measurement of primary stability (micro-motion): effect of bone density and insertion torque. *J Osteol Biomat.* 2010;1(3):141-149.
44. Hicklin SP, Schneebeli E, Chappuis V, Janner SFM, Buser D, Brägger U. Early loading of titanium dental implants with an intra-operatively conditioned hydrophilic implant surface after 21 days of healing. *Clin Oral Implants Res.* 2016;27(7):875-883.
45. Swami V, Vijayaraghavan V, Swami V. Current trends to measure implant stability. *J Indian Prosthodont Soc.* 2016;16(2):124.
46. Nedir R, Bischof M, Szmukler-Moncler S, Bernard JP, Samson J. Predicting osseointegration by means of implant primary stability. *Clin Oral Implants Res.* 2004;15(5):520-528.
47. Friberg B, Sennerby L, Meredith N, Lekholm U. A comparison between cutting torque and resonance frequency measurements of maxillary implants: a 20-month clinical study. *Int J Oral Maxillofac Surg.* 1999;28(4):297-303.
48. Gallucci GO, Benic GI, Eckert SE, et al. Consensus statements and clinical recommendations for implant loading protocols. *Int J Oral Maxillofac Implants.* 2013;29:287-290.
49. Winwood K, Zioupos P, Currey J, Cotton JR, Taylor M. The importance of the elastic and plastic components of strain in tensile and compressive fatigue of human cortical bone in relation to orthopaedic biomechanics. *J Musculoskelet Neuronal Interact.* 2006;6(2):134.
50. Bashutski JD, D'Silva NJ, Wang HL. Implant compression necrosis: current understanding and case report. *J Periodontol.* 2009;80(4):700-704.
51. Vafiadis D, Goldstein G, Garber D, Lambrakos A, Kowalski B. Immediate implant placement of a single central incisor using a CAD/CAM crown-root form technique: provisional to final restoration. *J Esthet Restor Dent.* 2017;29(1):13-21.

**How to cite this article:** Charatchaiwanna A, Rojsiraphisa T, Aunmeungtong W, Reichart PA, Khongkhunthian P. Mathematical equations for dental implant stability patterns during the osseointegration period, based on previous resonance frequency analysis studies. *Clin Implant Dent Relat Res.* 2019;1-13. <https://doi.org/10.1111/cid.12828>